A Design and Fabrication Approach for Pneumatic Soft Robotic Arms Using 3D Printed Origami Skeletons

K. Zhang[1,2], Y. Zhu[1], C. Lou[1], P. Zheng[1] and M. Kovač[1,3]

***Abstract*— Soft robots which employ materials with inherent compliance have demonstrated great potential in a variety of applications such as manipulators, medical tools and wearable devices. This paper presents an origami-folding inspired design and fabrication approach for developing semi-soft robotic arms. The approach starts from a conceptual design by identifying foldable origami structures. This is followed by the kinematic modelling of the selected origami skeleton with base folds of thick panels and flexible hinges. The final step realizes the design by 3D printing the skeleton and laminating the skeleton to flexible membranes on a heated vacuum table. Following the proposed approach, a foldable origami tube structure is designed, modelled and used as the exoskeleton for a pneumatic semi-soft robotic arm. Prototypes are developed by laminating a pair of 3D printed thermoplastic polyurethane (TPU) origami skeleton structures with TPU fabric film. The soft arm is actuated by a vacuum pump and its performances is evaluated through quasi-static tests. Experimental results show that the soft robotic arm achieves a maximum contraction ratio of 47.53% providing 23.463 N axial tension force when applying a regulated negative pressure of −1 bar. Two extensible and foldable pneumatic arms are integrated on a micro aerial vehicle (MAV) to obtain a platform with the potential of aerial manipulation capabilities in confined and hard to reach areas.**

I. INTRODUCTION

The field of soft robotics experiences a fast growing era with many soft robots [1], [2], [3] being developed to perform tasks in scenarios where conventional rigid-bodied robots are considered as not appropriate [4], [5]. The compliance of soft robots enabled by flexible materials leads to potential adaptability and increased robustness but it also brings new challenges in design, fabrication and control [6], [7], [8], [9]. One of the key challenges is to model and control the motion as well as the stiffness of soft robots. Recent investigations in this field demonstrated that augmented skeletons are capable of enhancing performances of the soft-bodied robotic systems in certain directions [9], [10], [11], [12]. For example, the integrated origami structure is able to not only effectively fold an artificial muscle [13] in a compact configuration but also largely help the muscle to gain stresses in the contraction direction when it is inflated. Simultaneously, the foldable origami structure can provide softness when the muscle is not fully contracted.

Folded morphologies are widely detected in nature of plants, animals, and insects. For instance, petals are folded inside of buds [14] and some insects fold their wings into carapaces [15]. Origami (an art of paper folding which originated in ancient Asia) shares certain properties of foldability of living systems and it offers excellent potentials for folding engineering designs. For example, organised spatially folds of paper to achieve required functions such as building specific shapes to make ornaments and toys, creating a storage state to save space, and introducing strength and stiffness to paper. These origami features are effective approaches to develop required morphology and function as well as save space and weight [16].

Origami-folding techniques have been sources of inspiration for engineers finding innovative solutions of problems in medicine, architecture, robotics and other fields [17], [18], [19]. Introducing folds to thin paper sheets not only can lead to self-interaction and added stiffness [20], but it can also result in various foldable and bendable mechanisms which can be adopted in designs of novel robotic systems. For instance, a twisting tower origami structure from Kresling crease pattern has been used for a crawling robot [21] and the Tachibana pattern twisted tower [22] has been employed in a three-fingered manipulator. Further, a Yoshimura pattern origami shell has been used to reinforce specific bending resilience of a soft pneumatic actuator [23]. Recently, cyclic Miura-ori was used in a novel impact protection system for robotic rotorcraft [24].

For the purpose of actuating the robotic systems with origami structures, various actuation systems have been explored in the recent years. Apart from piezoelectric materials, shape memory alloys, shape memory polymers, electromagnetic motors, pneumatic channels (for those origami robotics at centimetre scale and above) [25], [16], [22], pneumatic bag actuator and air pouch motors connected in series were developed for operating pneumatic arms and folding acrylic sheets into a structure [26].

The origami-folding inspired structures with foldability [27], [28] and lightweight structure have been found particular useful for aerial robots [29], [16], since most of the aerial robots including the Micro Aerial Vehicles (MAVs) have very limited payload and any added weight leads to higher energy consumption and shortened flight time [30].

In this work, we propose an origami-folding inspired design and fabrication approach for developing soft robotic arms. A novel pneumatic soft arm is developed by laminating

*This work was partially supported by research awards from the Engineering and Physical Sciences Research Council (EPSRC) under grant agreements EP/N018494/1, EP/R026173/1, EP/R009953/1 and EP/R02572X/1. Mirko Kovač is supported by the Royal Society Wolfson Fellowship under grant agreement RSFR1180003.(*Ketao Zhang and Yifan Zhu are co-first authors*)

[1] Aerial Robotics Lab, Department of Aeronautics, Imperial College London m.kovac@imperial.ac.uk

[2] School of Engineering and Material Science, Queen Mary University of London ketao.zhang@qmul.ac.uk

[3] Materials and Technology Centre of Robotics, Swiss Federal Laboratories for Materials Science and Technology (Empa)

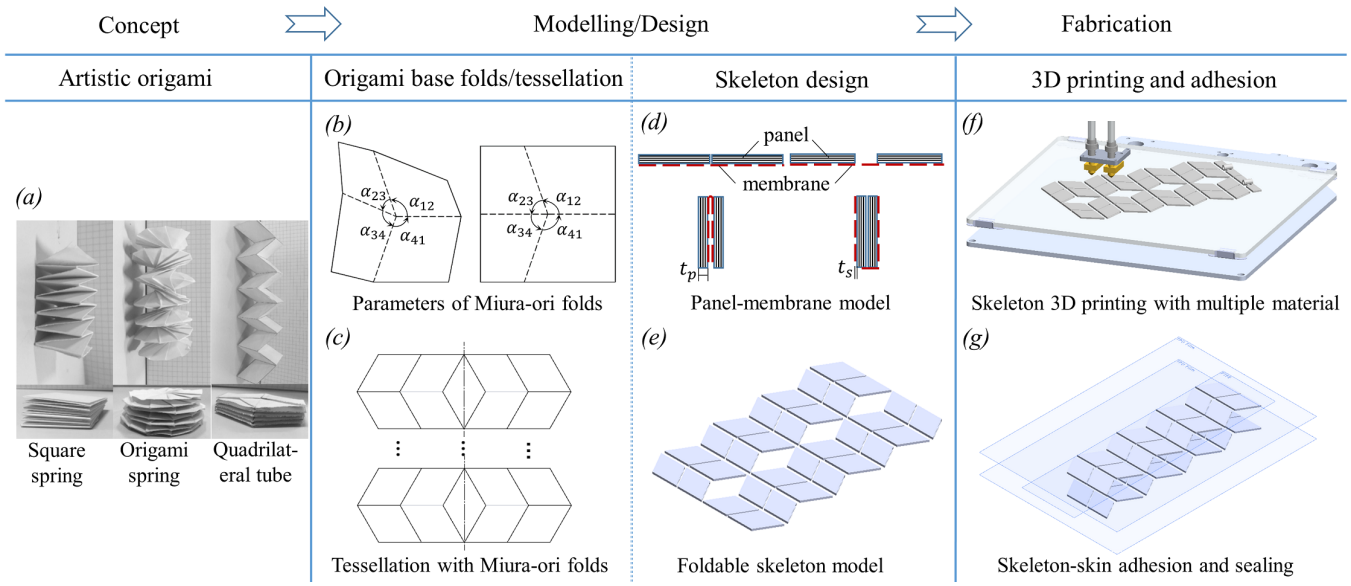

Fig. 1. Steps of the proposed approach for design, modelling and fabrication of pneumatic soft arms with origami exoskeleton (a) foldable origami structures in deployed and compact configurations: Square spring (left), Origami spring (middle) and Quadrilateral tube (right), (b) base folds examples of foldable origami [31], (c) origami tessellations with multiple base folds, (d) panel-membrane model [32] for mountain and valley folds of thick-panel origami structures, (e) design of the 2D mapping of foldable origami structure with thick panels, (f) 3D printing the origami skeleton using printable model material and dissolvable support material, (g) adhering skeleton to membrane and sealing layered membrane.

3D printed TPU origami skeleton and TPU fabric skin. A pair of soft arms were then integrated with a MAV demonstrating potentials to develop soft aerial robots towards aerial manipulation. This work contributes the following

1) The kinematics modelling based design approach of foldable origami skeleton.
2) The integrated fabrication process for flat laminating TPU fabric skin and 3D printed origami exoskeletons as well as creating air pockets in between TPU fabric layers for pneumatic actuation.
3) Light-weight pneumatic soft arms capable of a large extension and contraction ratio.

In the following sections, we first introduce the general design and fabrication approach for pneumatic soft robotic arms with origami exoskeleton. Following this general methods, section III presents the geometric and kinematic modelling of one example origami skeleton for a pneumatic soft robotic arm. Section IV will detail the fabrication steps of making the skeleton using 3D printing and the pneumatic arm by flat laminating in heated vacuum table. With the prototypes, section V will report the performance evaluation results and demonstrate the potential integration with aerial robots towards aerial manipulation, and the paper is then concluded in Section VI.

II. A Design and Fabrication Approach for the Origami-inspired Soft Robotic Arm

Origami has been an unique sculptural art evolving from simple paper folds to the more complicated modern origami with delicate crease patterns in a variety of flexible ways. The recently development of origami-folding inspired artificial systems shown that origami-folding in artistic discipline provides a source for catalysing interdisciplinary ideas thus exploring new solutions for certain engineering problems. Engineering design of articulated systems can draw inspiration from shapes and functions of origami artworks realised by arranging a sequence of folds. In particular, the creases on paper and thin sheets of origami structures acting as soft hinges extend another dimension for design and making of soft robots.

Starting from the essential principles of origami-folding, here we propose a kinematic modelling, 3D printing and lamination-based approach for developing pneumatic soft robotic arms with origami skeletons. This approach consists of three main phases (as illustrated in Fig. 1) which are further decomposed into seven steps and illustrated with a quadrilateral origami tube, as an implementation example. The steps include

1) Conceptual design and model selection of foldable artistic origami structures (Fig. 1(a)).
2) Geometric modelling of 2D origami base folds (Fig. 1(b)) corresponding to unit elements and kinematic folding motion analysis.
3) The complete mapping of the 2D crease pattern/tessellation (Fig. 1(c)) of the full origami skeleton for 3D folding motion.
4) Design of the panel-membrane model [32] for mountain and valley folds (Fig. 1(d)) in various modules/units of the foldable origami skeleton with consideration of panel thickness.
5) Completed design of the origami skeleton in 2D (Fig. 1(e)) considering the coupling and integration with actuation systems, such as for example the fluid inlet orifice.

6) 3D printing of the origami skeleton using build and water-soluble support materials and printers with reliable dual extrusion (Fig. 1(f)).
7) Lamination of the origami exoskeleton and soft membrane on a heat vacuum table to create the air pocket within the arm (Fig. 1(g)) and final integration with the actuation systems, such as a vacuum pump for pneumatic arms.

III. The Quadrilateral Origami Exoskeleton for the Pneumatic Soft Robotic Arm

The design concept in this paper is to use the approach above to develop a foldable soft robotic arm as a module for an integrated robotic end-effector, where the module is able to contract to a compact configuration for storage and a fully extended configuration for operation.

There are a large number of foldable origami structures such as the square spring [33], origami spiral [34] and the quadrilateral tube [35], [36], [37] (Fig. 1(a)), which can be folded and deployed in the axial direction of the structures. In the conceptual design stage, complexity of the folding steps, the stiffness of the structure, reconfigurability, and fabrication process using flat lamination are the design criteria for the origami structure. The quadrilateral tube (Fig. 2) is selected as an example for demonstrating the kinematics based design and fabrication approach proposed in this paper.

A. Geometric modelling of the origami quadrilateral tube

The artistic origami quadrilateral tube (Fig. 2(a)) can be quickly produced by folding a piece of flat paper [37] with 2D crease pattern in Fig. 2(b). In the 2D crease pattern, solid lines indicate *mountain creases* folding outward, dotdash lines are *valley creases* folding inward, dashed lines indicate cutting lines, and the square blocks are adhesive flaps.

The quadrilateral tube consists of five identical modules and each module (Fig. 2(c)) has two elements which are symmetric with the plane defined by vertices A_I, B_I, C_I and D_I. The four creases of each element keep parallel during the folding motion. In order to analyse the motion of the origami tube, a right-handed local coordinate frame of the module is defined with the origin attached to the vertex A_I. Its x axis passes C_I, with the y axis perpendicular to the symmetric plane and the z axis defined by the right-hand-rule (Fig. 2(c)).

The 2D crease base of each module (Fig. 2(b)) is symmetric with the line defined by A_I, B_I, C_I and D_I. The geometry of the crease base is defined by three parameters, which are the length of creases denoted by a and b and the angle α_0. As illustrated in the 3D module, the distance between the top cross section defined by vertices A_{II}, B_{II}, C_{II} and D_{II} and the bottom cross section by vertices A_I, B_I, C_I and D_I is defined as the height of each element and it is denoted by h. The angle measured from the bottom cross section to the mountain crease A_IA_{II} is denoted by α and the angle measured from $x-$axis to crease A_ID_I by β.

While the origami tube is in folding action, the measures α, β and h are varying and the geometric relationship is given by

$$\alpha = \sin^{-1}(h/b) \tag{1}$$

and

$$\cos\alpha\cos\beta = \cos\alpha_0 \tag{2}$$

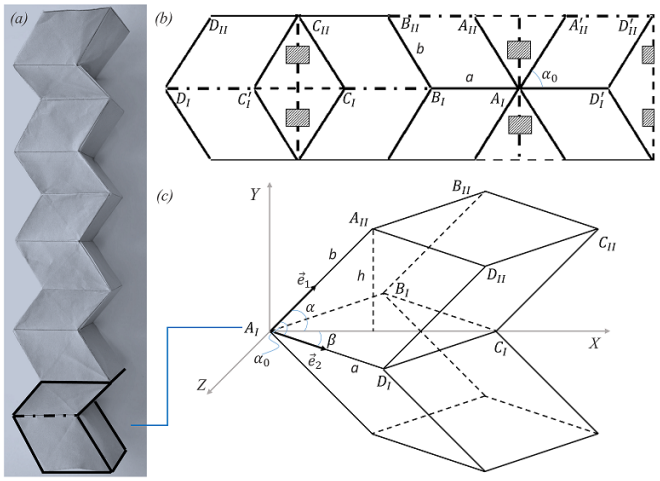

Fig. 2. The origami quadrilateral tube and its crease pattern for one module. (a) The extended origami tube consists of 10 elements in 5 modules, with coloured creases for one module, (b) the 2D crease pattern for one module consists of two elements symmetric with the cross section, (c) geometric model of the module.

B. Kinematics Analysis of the Origami Tube

For an origami tube structure with design parameters $\alpha_0 = 60°$, and $a = b = 20$mm, the angle α is within the range $[0, 60°]$ and the relationship between the height h and angles α and β is plotted in Fig. 3(a). While the motion path of vertices of the element is illustrated in Fig. 3(b).

The inside volume, $V(\alpha,\beta)$, of the origami tube is varying in the process of folding and is expressed as

$$V(\alpha,\beta) = a^2 b\sin\alpha\sin 2\beta \tag{3}$$

In the compact folded condition when all layers are compressed, i.e. $h = 0$, the volume $V(\alpha,\beta) = 0$. Applying the method of Lagrange multipliers with Eq. 2 as a single constraint, the Lagrange function is expressed as

$$F(\alpha,\beta,\lambda) = a^2 b\sin\alpha\sin 2\beta - \lambda\left(\cos\alpha_0 - \cos\alpha\cos\beta\right) \tag{4}$$

The tube configuration with the maximum volume is then obtained by solving

$$\nabla_{\alpha,\beta,\lambda} F(\alpha,\beta,\lambda) = 0. \tag{5}$$

The solutions are

$$\alpha = \cos^{-1}\sqrt{\frac{2\cos^2\alpha_0}{1+\cos^2\alpha_0}} \tag{6}$$

$$\beta = \cos^{-1}\sqrt{\frac{1}{2\left(1+\cos^2\alpha_0\right)}} \tag{7}$$

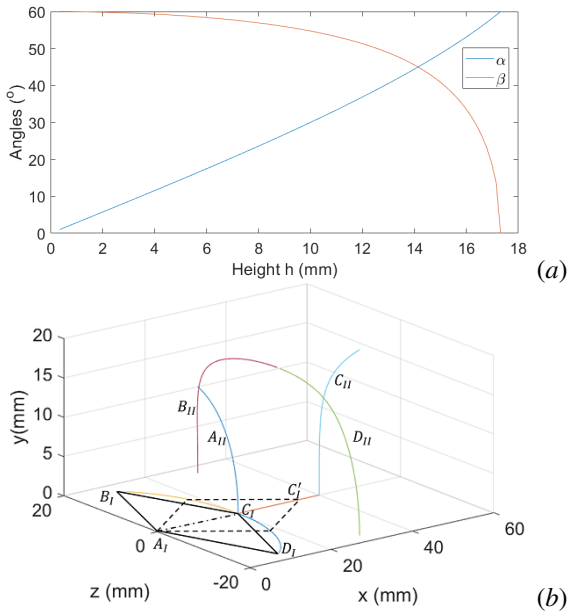

Fig. 3. Folding motion of the single element in each module for straight line contraction and extension. (a) geometric relationship between height h and angles α and β, (b) motion path of all vertices of a single element and the cross section corresponding to compact and maximum volume configurations.

This reveals that a quadrilateral tube with the design parameters $\alpha_0 = 60^\circ$ and $a = b = 20$ mm reaches its maximum volume when $\alpha = 50.77^\circ$ and $\beta = 37.76^\circ$. When the tube deploys from the fully compact configuration to the maximum volume configuration, the parallelogram defined by A_I, B_I, C_I and D_I in Fig. 3(b) changes to a shape where $\beta = 37.76^\circ$ (dashed line defined by A_I, B_I', C_I' and D_I').

C. Skeleton 2D Design

In the traditional art of origami made from thin paper, the thickness of the paper doesn't affect the folding. However, thick panel origami structures [38] have to be accommodated the thickness of panels by adding gap distances between panels in the 2D pattern, thus allowing the desired folding motion and leading to final folded compact configuration.

Evolving the origami structure in Fig. 2 to a foldable skeleton, we introduce two more design parameter, panel thickness t_p and skin thickness t_s in addition to the three geometric parameters a and b and the angle α_0 for accommodating the thickness of panels during folding motion. Following the panel-membrane model [32], the gap for mountain creases is denoted by g_m and that for valley crease by g_v in the 2D model of the skeleton in Fig. 4. To achieve 180° valley fold, the gaps corresponding to mountain and valley creases are $g_m = 2t_s$ and $g_v = 2t_p + 4t_s$.

In order to minimize the creases to be regenerated during the fabrication process, the original crease pattern in Fig. 4(a) is modified by moving panels of the right column to the left. This results in a line symmetric origami structure accommodating panel thickness (Fig. 4(b)). For the purpose of sealing, a gap is added along the symmetric line (dashed line in Fig. 4(b)) of the pattern and the distance is marked as g_s.

As illustrated in Fig. 3(b), the angle α and the cross section $A_IB_IC_ID_I$ are varying in the folding process of the tube structure. Considering these properties while folding the tube, a coupler for integrating the foldable arm with mounting frame is proposed. The coupler is a parallelogram four-bar linkage, with the length of all links being defined by the crease length a of the skeleton structure. With such a coupler, the hinge passing vertex B_I is rotating along a fixed axis perpendicular to the cross section plane. The other three hinges are moving with the hinge passing vertex D_I is sliding along the line defined by B_1D_1 (Fig. 3(b) and Fig. 4). Adding the four-bar linkage to the 2D skeleton, the final 3D printed skeleton is illustrated in Fig. 4(b).

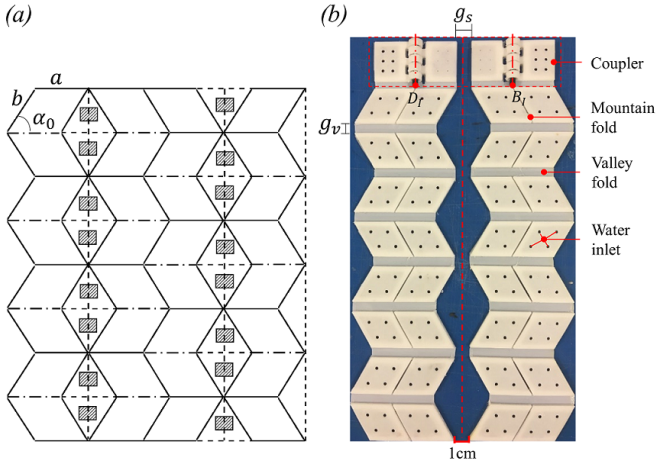

Fig. 4. 2D design and 3D printed prototype of the origami skeleton. (a) 2D crease pattern of the skeleton, (b) the 3D printed thick origami skeleton with a four-bar linkage coupler using Ultimaker white TPU 95A and PVA filaments.

IV. Fabrication of the Soft Arm: Skeleton 3D Printing and Skin Adhesion

Multi-material additive-manufacturing techniques which allow materials with different mechanical properties to be placed at arbitrary locations within a structure are transforming conventional fabrication approaches for a wide range of products. In particular, 3D printing using soft materials has been demonstrated as a cost effective approach for developing both rigid and soft robotic systems [39], [40]. This section presents the 2D design of the skeleton, the 3D printable material selection for the origami skeleton and the adhesion procedure using TPU fabric as the skin of the arm.

We use a commercial 3D printer, the Ultimaker 3, with dual 0.4mm nozzles to print the skeleton structure. Model materials including Nylon (flexible, durable, corrosion-resistant), ABS (tough, stable, impact-resistant), and TPU 95A (semi-flexible and resistant to wear and tear) are used for the testing model, while PVA (water-soluble material) is chosen as the support material to be dissolved through water inlet (Fig. 4(b)) once the structure is printed.

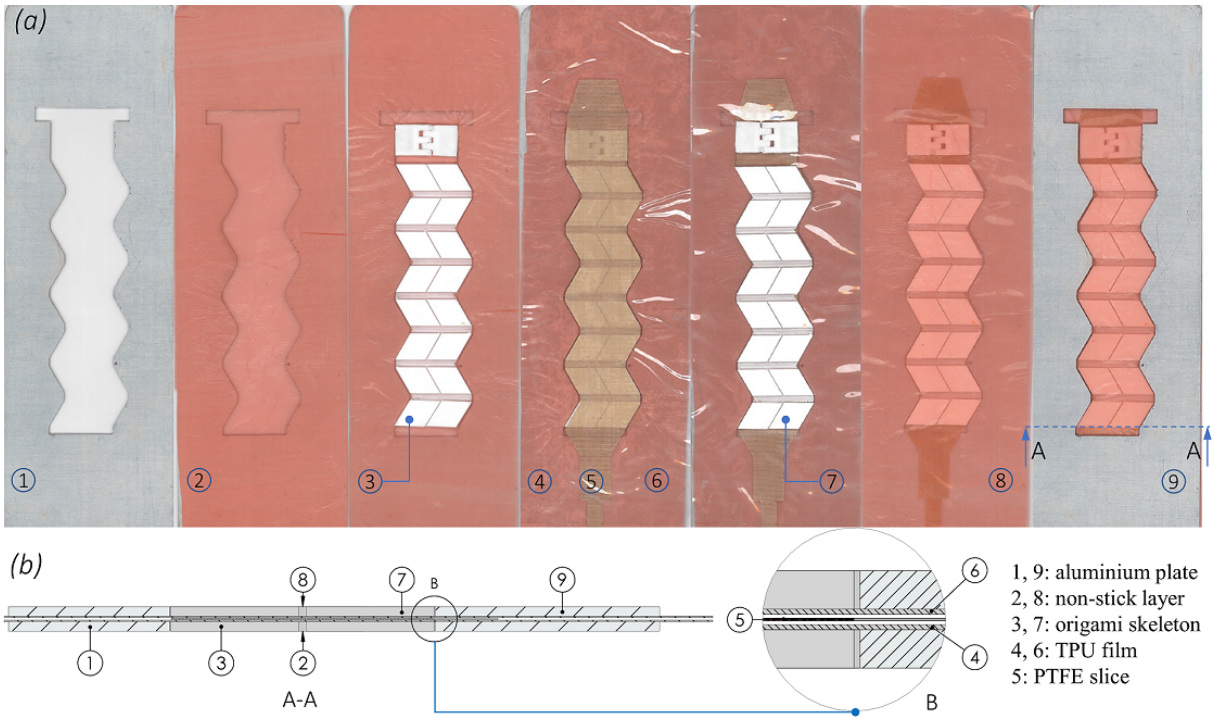

Fig. 5. Stacking order of 3D printed skeleton and films for adhesion and sealing. (a) top view of the staking sequence of all components including bottom (1) and top (9) aluminium plates with cut out in the shape of the skeleton, non-stick material layers (2) and (8), 3D printed skeletons (3) and (7), TPU films (4) and (6), and PTFE slice (5), (b) the cross-section view (A-A) and detail view (B) of the staking sequence of all components in layers.

Considering both mechanical properties and compatibility with other materials, air tight TPU film can be used the skin of air pockets in the arm. A sample of a selected commercial TPU fabric film was analysed by a standard experiment of the differential scanning calorimetry (DSC). A thermogram from 25 °C to 300 °C at a heating rate of 10 °C/min is exported from a Mettler Toledo DSC 3. The experimental results provide a crystallisation temperature of 156 °C and a melting point of 260 °C of the TPU film. These two values indicate the appropriate welding temperature of the film to be in the range of $[156, 260]$ °C.

The foldablility of 3D printed skeletons printed with various materials and the welding temperature of TPU fabric film are tested for identifying the best setting for fabricating the arm. The results shown that skeletons printed using Ultimaker TPU95A preserve best foldability.

To test the adhesion quality of the skeleton and skin, a series of welding tests with temperature between 120 °C to 200 °C (at 20 °C temperature interval) were implemented. Based on these tests, the optimal process is identified as (*i*) preheating the table to $[150, 160]$ °C and (*ii*) vacuuming the table to -0.9 bar for $[2, 5]$min.

The final step of the fabrication process is to seal the open creases in an heated vacuum table thus forming an enclosure air pocket inside the TPU skin. To create the air pocket between the two layers of TPU skin in the welding and sealing process, a non-stick PTFE slice was cut following the contour line of the skeleton and subsequently being inserted between the two layers of TPU skin. Further, a pair of 2 mm thick aluminium plates (Fig. 5(a)) were cut following the skeleton profile and then used to embed the skeleton and provide flat surface for the TPU film. As illustrated in Fig. 5, the printed skeleton, TPU films and PTFE slice are then laid in stacking order of 'non-stick sheet - skeleton - TPU film - PTFE slice - TPU film - skeleton - non-stick sheet' and sandwiched between the bottom and top aluminium sheets. This leads to a stacked mould (Fig. 5(b)) which is then placed in the heat vacuum table for completing the adhesion and sealing process. The PTFE slice is subsequently taken out of the arm after the adhesion stage. As long as this fabrication process is completed, a Self-Sealing-Tee [41] is assembled for the purposa of connecting the pneumatic actuation system. A thin TPU strip is added inside the soft arm for adjusting the initial configuration by clamping the TPU skin and the strip tightly with two clips at the end of the arm. For the soft arm in Fig. 6, the initial configuration is set at the length (L_{max}) corresponding to its maximum volume. The mass of the foldable soft pneumatic arm with 3D printed origami exoskeleton is 69.15 g.

V. Performance Characterization of the Pneumatic Soft Arm

This section reports the experimental characterization and test results of the soft arm. The test setup consists of a station vacuum pump which provides regulated pressures for retracting the arm from the initial configuration to a final compact configuration.

We characterize the force and contraction performances of the proposed pneumatic soft arm through a series of

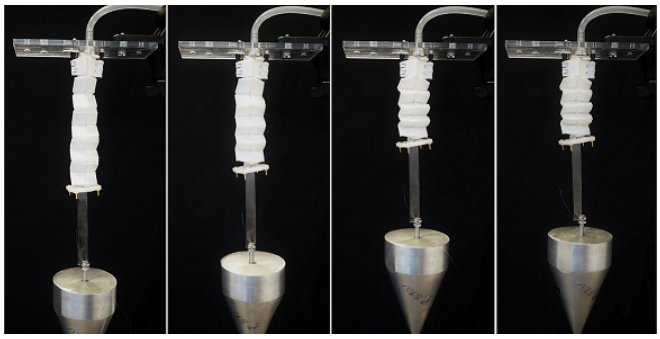

Fig. 6. Sequential folding progress from the original configuration to the compact configuration during quasi-static tests. The pneumatic soft arm actuated with regulated pressure of a station vacuum pump.

quasi-static tests (Fig. 6) by applying various pressure levels. As shown in Fig. 7, the average maximum lifting force of 4.224 N, 10.948 N, 16.43432 N, 20.213 N and 23.463 N were generated using regulated pressure at 0.2 bar, −0.4 bar, −0.6 bar, −0.8 bar and −1.0 bar, respectively. The time spent to fully retract the soft arm without any payload is 1.5 seconds on average. The length of arm at its fully retracted stage is 47.53% of the length at maximum volume.

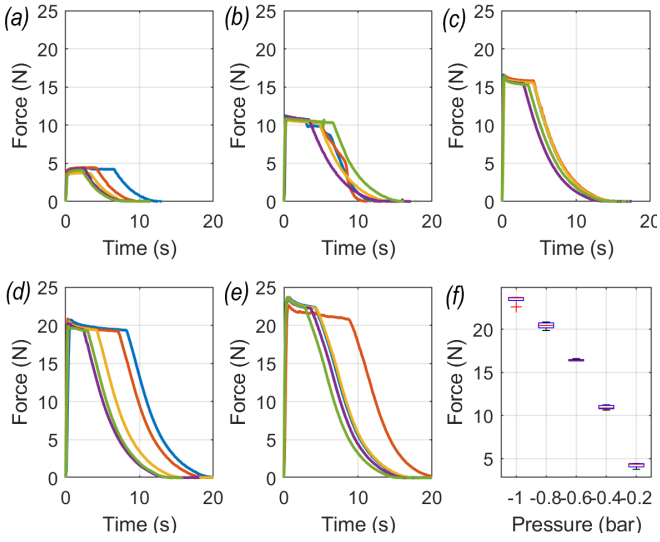

Fig. 7. The lift forces generated using regulated negative pressure of (a) 0.2 bar, (b) −0.4 bar, (c) −0.6 bar, (d) −0.8 bar, (e) −1.0 bar generated by a stationary pump, (f) box plot of peak forces using above pressure.

The soft pneumatic arm has distinct advantages such as light-weight, foldability and deployability. Further, the softness enabled by the flexible TPU fabric skin and semi-soft panels of the 3D printed skeleton could allow the pneumatic arm performing safety critical tasks around delicate objects. Building on these advantages, the lightweight foldable arm suits well the requirements for integrated aerial robots towards applications such as aerial inspection and manipulation. We demonstrated the concept of aerial robot with soft arms by integrating two soft arms with an quadrotor as in Fig. 8. Given the limited payload of the quadrotor Micro Aerial Vehicle (MAV), a compact BOXER 3KD DC pump (Fig. 8(a)) is mounted on the MAV and used to actuate the dual pneumatic arms. The characterisation of the integrated aerial robotic system (Fig. 8(b)) with dual soft arms is beyond the scope of this paper and can be investigated by focusing on control contributions related to aerial manipulation.

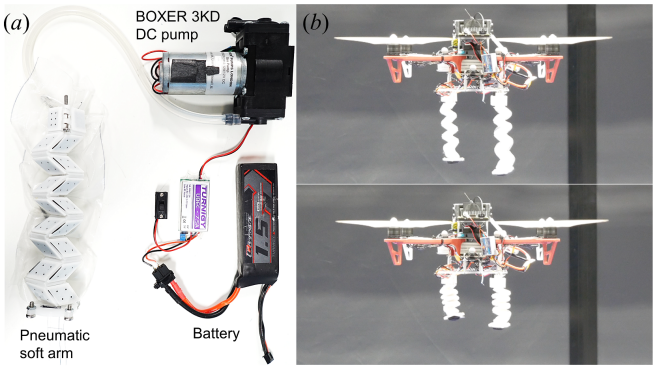

Fig. 8. The pneumatic soft arm and an integrated MAV platform with dual soft arms. (a) The pneumatic soft arm with a light-weight double headed gas diaphragm pump as actuator, (b) the MAV with two integrated soft arms in extended and folded configurations respectively actuated by an on-board pump.

VI. CONCLUSIONS

This paper presentes a design and fabrication approach for developing foldable soft robotic arms with 3D printed origami skeletons. The seven-step approach combines conceptual design, kinematic modelling, as well as 3D printing and thermal lamination based fabrication phases. Following the proposed approach, two pneumatic soft arms were produced by using 3D printed quadrilateral tubes as the foldable exoskeleton and TPU fabric film as skin. The soft robotic arm is able to achieve a 47.53% contraction ratio and it provides 23.463 N axial tension force at a negative pressure of −1 bar. In addition, the use of pneumatic actuation system offers short activating times of the robotic arm. For example, the arm changes from the maximum volume configuration to the final compact configuration in 1.5 seconds.

The proposed design and fabrication approach is beneficial to scalability of size and forces and thus adaptable to different working conditions. The combination of technologies including 3D printing with soft filament and thermal lamination provides a cost effective approach for making foldable soft robotic devices based on additive manufacturing.

Future work will further explore static performance of the soft arm itself without actuation and stiffness control of the robotic arm by regulating the pressure input. We will further explore potentials of aerial manipulation using pneumatic soft arms presented in this paper.

REFERENCES

[1] M. T. Tolley, R. F. Shepherd, B. Mosadegh, K. C. Galloway, M. Wehner, M. Karpelson, R. J. Wood, and G. M. Whitesides, "A resilient, untethered soft robot," *Soft robotics*, vol. 1, no. 3, pp. 213–223, 2014.

[2] R. Deimel and O. Brock, "A novel type of compliant and underactuated robotic hand for dexterous grasping," *The International Journal of Robotics Research*, vol. 35, no. 1-3, pp. 161–185, 2016.

[3] H. Zhao, K. OBrien, S. Li, and R. F. Shepherd, "Optoelectronically innervated soft prosthetic hand via stretchable optical waveguides," *Science Robotics*, vol. 1, no. 1, p. eaai7529, 2016.

[4] J. Fras and K. Althoefer, "Soft biomimetic prosthetic hand: Design, manufacturing and preliminary examination," in *2018 IEEE/RSJ International Conference on Intelligent Robots and Systems (IROS)*, Oct 2018, pp. 1–6.

[5] A. Albu-Schaffer, O. Eiberger, M. Grebenstein, S. Haddadin, C. Ott, T. Wimbock, S. Wolf, and G. Hirzinger, "Soft robotics," *IEEE Robotics & Automation Magazine*, vol. 15, no. 3, 2008.

[6] L. Margheri, C. Laschi, and B. Mazzolai, "Soft robotic arm inspired by the octopus: I. from biological functions to artificial requirements," *Bioinspiration & biomimetics*, vol. 7, no. 2, p. 025004, 2012.

[7] C. Majidi, "Soft robotics: a perspectivecurrent trends and prospects for the future," *Soft Robotics*, vol. 1, no. 1, pp. 5–11, 2014.

[8] M. Kovač, "The bioinspiration design paradigm: A perspective for soft robotics," *Soft Robotics*, vol. 1, no. 1, pp. 28–37, 2014.

[9] D. Rus and M. T. Tolley, "Design, fabrication and control of soft robots," *Nature*, vol. 521, no. 7553, p. 467, 2015.

[10] A. Firouzeh and J. Paik, "Robogami: A fully integrated low-profile robotic origami," *Journal of Mechanisms and Robotics*, vol. 7, no. 2, p. 021009, 2015.

[11] M. Salerno, K. Zhang, A. Menciassi, and J. S. Dai, "A novel 4-dof origami grasper with an sma-actuation system for minimally invasive surgery," *IEEE Transactions on Robotics*, vol. 32, no. 3, pp. 484–498, 2016.

[12] K. Zhang, C. Qiu, and J. S. Dai, "An extensible continuum robot with integrated origami parallel modules," *Journal of Mechanisms and Robotics*, vol. 8, no. 3, p. 031010, 2016.

[13] S. Li, D. M. Vogt, D. Rus, and R. J. Wood, "Fluid-driven origami-inspired artificial muscles," *Proceedings of the National Academy of Sciences*, vol. 114, no. 50, pp. 13 132–13 137, 2017.

[14] P. Melgarejo, R. Martínez-Valero, J. Guillamón, M. M. AMORÓS, and A, "Phenological stages of the pomegranate tree (punka granatum l.)," *Annals of applied biology*, vol. 130, no. 1, pp. 135–140, 1997.

[15] K. Saito, S. Nomura, S. Yamamoto, R. Niiyama, and Y. Okabe, "Investigation of hindwing folding in ladybird beetles by artificial elytron transplantation and microcomputed tomography," *Proceedings of the National Academy of Sciences*, vol. 114, no. 22, pp. 5624–5628, 2017.

[16] S.-J. Kim, D.-Y. Lee, G.-P. Jung, and K.-J. Cho, "An origami-inspired, self-locking robotic arm that can be folded flat," *Science Robotics*, vol. 3, no. 16, p. eaar2915, 2018.

[17] S. Miyashita, S. Guitron, K. Yoshida, S. Li, D. D. Damian, and D. Rus, "Ingestible, controllable, and degradable origami robot for patching stomach wounds," in *Proceedings-IEEE International Conference on Robotics and Automation*, vol. 2016. Sheffield, 2016, pp. 909–916.

[18] T. Tachi, "Rigid-foldable thick origami," *Origami*, vol. 5, pp. 253–264, 2011.

[19] J. A. Faber, A. F. Arrieta, and A. R. Studart, "Bioinspired spring origami," *Science*, vol. 359, no. 6382, pp. 1386–1391, 2018. [Online]. Available: http://science.sciencemag.org/content/359/6382/1386

[20] E. T. Filipov, T. Tachi, and G. H. Paulino, "Origami tubes assembled into stiff, yet reconfigurable structures and metamaterials," *Proceedings of the National Academy of Sciences*, vol. 112, no. 40, pp. 12 321–12 326, 2015.

[21] A. Pagano, T. Yan, B. Chien, A. Wissa, and S. Tawfick, "A crawling robot driven by multi-stable origami," *Smart Materials and Structures*, vol. 26, no. 9, p. 094007, 2017.

[22] D. Jeong and K. Lee, "Design and analysis of an origami-based three-finger manipulator," *Robotica*, vol. 36, no. 2, pp. 261–274, 2018.

[23] L. Paez, G. Agarwal, and J. Paik, "Design and analysis of a soft pneumatic actuator with origami shell reinforcement," *Soft Robotics*, vol. 3, no. 3, pp. 109–119, 2016.

[24] P. Sareh, P. Chermprayong, M. Emmanuelli, H. Nadeem, and M. Kovac, "Rotorigami: A rotary origami protective system for robotic rotorcraft," *Science Robotics*, vol. 3, no. 22, p. eaah5228, 2018.

[25] D. Rus and M. T. Tolley, "Design, fabrication and control of origami robots," *Nature Reviews Materials*, p. 1, 2018.

[26] H.-J. Kim, A. Kawamura, Y. Nishioka, and S. Kawamura, "Mechanical design and control of inflatable robotic arms for high positioning accuracy," *Advanced Robotics*, vol. 32, no. 2, pp. 89–104, 2018.

[27] L. Dufour, K. Owen, S. Mintchev, and D. Floreano, "A drone with insect-inspired folding wings," in *Intelligent Robots and Systems (IROS), 2016 IEEE/RSJ International Conference on*. Ieee, 2016, pp. 1576–1581.

[28] S. Mintchev, J. Shintake, and D. Floreano, "Bioinspired dual-stiffness origami," *Science Robotics*, vol. 3, no. 20, p. eaau0275, 2018.

[29] S. Sareh, R. Siddall, T. Alhinai, and M. Kovac, "Bio-inspired soft aerial robots: adaptive morphology for high-performance flight," in *Soft Robotics: Trends, Applications and Challenges*. Springer, 2017, pp. 65–74.

[30] M. Kovac, "Learning from nature how to land aerial robots," *Science*, vol. 352, no. 6288, pp. 895–896, 2016.

[31] K. Miura, "Method of packaging and deployment of large membranes in space," *Title The Institute of Space and Astronautical Science Report*, vol. 618, p. 1, 1985.

[32] S. A. Zirbel, R. J. Lang, M. W. Thomson, D. A. Sigel, P. E. Walkemeyer, B. P. Trease, S. P. Magleby, and L. L. Howell, "Accommodating thickness in origami-based deployable arrays," *Journal of Mechanical Design*, vol. 135, no. 11, p. 111005, 2013.

[33] pinheadj17. (2011, Nov. 5) How to make paper spring. [YouTube video]. Accessed Sept. 20, 2018. [Online]. Available: https://youtu.be/voHi98IcTyQ

[34] Jo Nakashima. (2012, Sept. 20) Origami spring into action (jeff beynon). [YouTube video]. Accessed Sept. 20, 2018. [Online]. Available: https://youtu.be/aul0SzPVsls

[35] E. T. Filipov, T. Tachi, and G. H. Paulino, "Origami tubes assembled into stiff, yet reconfigurable structures and metamaterials," *Proceedings of the National Academy of Sciences*, vol. 112, no. 40, pp. 12 321–12 326, 2015.

[36] Y. Chen, W. Lv, J. Li, and Z. You, "An extended family of rigidly foldable origami tubes," *Journal of Mechanisms and Robotics*, vol. 9, no. 2, p. 021002, 2017.

[37] NeoSpica Paper Structures. (2015, Jun. 2) Tutorial 24 - eggbox sheet folding collapsible in x and y rigid in z. [YouTube video]. Accessed Sept. 10, 2018. [Online]. Available: https://youtu.be/5pfcg4AuVJ4

[38] Y. Chen, R. Peng, and Z. You, "Origami of thick panels," *Science*, vol. 349, no. 6246, pp. 396–400, 2015.

[39] R. MacCurdy, R. Katzschmann, Y. Kim, and D. Rus, "Printable hydraulics: A method for fabricating robots by 3d co-printing solids and liquids," pp. 3878–3885, May 2016.

[40] K. Zhang, P. Chermprayong, D. Tzoumanikas, W. Li, M. Grimm, M. Smentoch, S. Leutenegger, and M. Kovac, "Bioinspired design of a landing system with soft shock absorbers for autonomous aerial robots," *Journal of Field Robotics*, vol. 0, no. 0. [Online]. Available: https://onlinelibrary.wiley.com/doi/abs/10.1002/rob.21840

[41] M. Motorsport, "Self Sealing Tee With 5mm Barbed Outlet," accessed 2018-10-10. [Online]. Available: https://www.merlinmotorsport.co.uk/p/self-sealing-tee-with-5mm-barbed-outlet-sst01